Modular poly(ethylene glycol) ligands for biocompatible semiconductor and gold nanocrystals with extended pH and ionic stability†

Bing C. Mei,[ab] Kimihiro Susumu,[a] Igor L. Medintz,[c] James B. Delehanty,[c] T. J. Mountziaris[b] and Hedi Mattoussi*[a]

Received 20th June 2008, Accepted 5th August 2008
First published as an Advance Article on the web 12th September 2008
DOI: 10.1039/b810488c

We describe the design of new ligands made by coupling commercially available poly(ethylene glycol) methyl ether (mPEG, HO-PEG-OCH_3) and thioctic acid (TA) *via* a stable amide bond to form TA-PEG-OCH_3 molecules. The ligands were obtained by a simple transformation of the hydroxyl group on the mPEG into an amine group, followed by attachment of TA *via* *N*,*N*′-dicyclohexylcarbodiimide (DCC) coupling. Following ring opening of the 1,2-dithiolane on the TA-PEG-OCH_3 to form a dihydrolipoic acid (DHLA) group, DHLA-PEG-OCH_3 was obtained. Cap exchange of nanoparticles with DHLA-PEG-OCH_3 provided dispersions in buffer solutions that were stable over a broad pH range (from 3 to 13 for CdSe-ZnS QDs and 2–13 for Au nanoparticles). Using DHLA-PEG-OCH_3 either neat or mixed with amine- or carboxyl-terminated ligands (DHLA-PEG-NH_2 or DHLA-PEG-COOH) allowed tuning of the surface functionalities of these nanoparticles. Microinjection of the ligand-exchanged QDs into live cells indicated that the newly capped QDs were stable and well dispersed in the cell cytosol for up to 32 h following delivery. The fluorescence distribution and its evolution over time of these DHLA-PEG-OCH_3-QDs indicate improved intracellular stability and reduced non-specific interactions compared to nanocrystals capped with DHLA-PEG-OH.

Introduction

Semiconductor nanocrystals (or quantum dots, QDs) and metallic nanoparticles have generated much interest in the past decade, due to their unique, tunable, spectroscopic properties and the ever-expanding range of potential applications.[1–10] Biological use of these nanoparticles (*e.g.*, QDs as fluorescent tags and Au nanoparticles as scattering labels) is particularly promising both for *in vivo* imaging of tissues and cells and for *in vitro* clinical diagnostics. Luminescent QDs, such as CdSe–ZnS core–shell nanocrystals, exhibit high photoluminescence quantum yields, large extinction coefficients, and strong resistance to photo- and chemical degradation.[6,8] Although there have been reports of QD synthesis in aqueous media (*e.g.*, growth in micelles), the highest quality materials are routinely synthesized by reacting organometallic precursors at high temperature in coordinating solvents consisting of mixtures of trioctylphosphine/trioctylphosphine oxide (TOP/TOPO) and alkyl amines.[11–16] Consequently, as-synthesized QDs are capped with hydrophobic ligands and are not dispersible in aqueous solutions. Since a large fraction of the total atoms are distributed on or near the nanoparticle surfaces, resulting in large surface-to-volume ratios, the capping ligands play a critical role in controlling their reactivity, as well as their chemical and colloidal stability. For QDs, it is also important to properly passivate the nanocrystals' surfaces in order to maintain their photoluminescence efficiency. Rendering these nanoparticles dispersible and stable in aqueous buffer solutions, while maintaining their optical properties, is critical for using them to develop biological applications.

Several strategies that yield aqueous dispersions of QDs have been reported in the past decade.[3,8] These methods can be grouped into two categories: (1) exchange of the native TOP/TOPO with hydrophilic ligands, usually comprised of anchor group(s) for binding to the nanocrystal surface at one end and hydrophilic groups at the other end, to promote solubility in aqueous solutions;[17–20] (2) encapsulating the as-synthesized QDs with amphiphilic molecules such as lipids or block co-polymers.[21–23] Surface ligand cap exchange can provide high quality water-soluble nanocrystals that are functional and more importantly, small in size. We have previously reported the design of hydrophilic ligands consisting of thioctic acid (TA) chemically coupled to a tunable poly(ethylene glycol) (PEG) segment *via* an esterification reaction. With this simple coupling chemistry, a set of hydroxy-terminated TA-PEG ligands was generated.[17] We found that following ring opening of the terminal dithiolane to produce a dithiol group, the resulting dihydrolipoic acid-appended ligands (DHLA-PEG-OH) allowed effective cap exchange of the QDs. Hydrophilic luminescent nanocrystals that are stable over a relatively broad range of pH values were thus

[a]*Division of Optical Sciences, Naval Research Laboratory, Washington, DC 20375, USA. E-mail: hedi.mattoussi@nrl.navy.mil*
[b]*Department of Chemical Engineering, University of Massachusetts, Amherst, MA 01003, USA*
[c]*Center for Bio/Molecular Science and Eng., Naval Research Laboratory, Washington, DC 20375, USA*

† Electronic supplementary information (ESI) available: Detailed synthesis procedure of all the intermediates and final compounds; luminescence of DHLA-PEG-OCH_3 cap-exchanged CdSe/ZnS QDs; additional cell micrographs (DIC and fluorescence). See DOI: 10.1039/b810488c

prepared. We have further expanded this synthetic design to make TA-based and DHLA-based PEG ligands that contain an amide linkage and specific functional end groups, including -NH_2, -COOH, and -biotin.[18] In that work, a short poly(ethylene glycol) segment (PEG400, MW ~400 Da) was used due to ease of implementation and purification. These ligands enable the use of common bioconjugation methods such as 1-ethyl-3-(3-dimethylaminopropyl)carbodiimide (EDC) coupling to attach biomolecules to QDs. The density of functional groups on the QD surface was tailored by incorporating a fraction of ligands that have an "inert" terminal end group. This was achieved by mixing hydroxy-terminated ligands (namely, DHLA-PEG600-OH as the majority ligand) with ligands having the desired end group to tune the functional valency of the QDs.[18] This is crucial as it allows potential control of the reactivity of the nanocrystal and the ligand valence of the final conjugate. Similar results were recently reported by the Bawendi group.[19]

However, while the hydroxy-terminated DHLA-PEG ligands have been effective in promoting water dispersion of CdSe–ZnS core–shell QDs, we have found that the necessary reduction step of the 1,2-dithiolane ring (using sodium borohydride, $NaBH_4$) to transform TA-PEG-OH to DHLA-PEG-OH can decompose the TA-PEG-OH if excess $NaBH_4$ is used, presumably due to the labile ester bond. In addition, the hydroxy group, while often assumed to be relatively inert, can react with certain functional groups commonly used for bioconjugation (*e.g.*, isocyanate).[24] For this reason, it would be advantageous to improve the design and prepare a robust alternative ligand that utilizes an amide linkage, rather than an ester, and presents an inert terminal function.

In this study, we address the above limitations and report the synthesis of a new bidentate ligand that is also based on the TA and PEG motifs. In this modified design, the ligands feature an amide bond, instead of an ester, to couple TA to poly(ethylene glycol) methyl ether and form TA-PEG-OCH_3, as shown in Fig. 1.[25] The poly(ethylene glycol) methyl ether (mPEG), which is commercially available, is terminated with a hydroxy group on one end and a methoxy group on the other. Since the mPEG precursor presents only one hydroxy group instead of two as in references 17 and 18, the synthetic scheme was also substantially improved and the purification steps readily simplified. Following synthesis and purification, we found that reduction of TA-PEG-OCH_3 to produce DHLA-PEG-OCH_3 (see Fig. 1) was unaffected by the concentration of $NaBH_4$ used (from 1 to 4 times molar excess). Furthermore, the presence of a methoxy terminal group instead of a hydroxy can potentially mitigate non-specific interactions, an issue of great importance in biological systems.[26,27] We also describe the preparation and purification of amine- and carboxyl-functionalized DHLA-PEG600 ligands, with additional improvements on the procedures as reported in reference 18. We found that QDs capped with these new ligands were stable over a broad range of pH values (from 3 to 13). Side-by-side comparison of intracellular microinjection of QDs capped with DHLA-PEG-OCH_3 and DHLA-PEG-OH indicated improvement in the dispersions of QDs capped with the new ligands inside the cell cytoplasm. The utility of the new ligands was further demonstrated with gold nanoparticles (AuNPs). AuNPs capped with these ligands were stable even at high salt concentrations and over a broad range of pH values (2–13).

Experimental

1. Materials and instrumentation

All air-sensitive materials were handled in a glovebox (MBraun Labmaster 130, Stratham, NH) and standard Schlenk techniques were used in the manipulation of air-sensitive materials. The syntheses were carried out under N_2 that passed through an O_2 scrubbing tower, unless otherwise stated. Poly(ethylene glycol) (average molecular weight 600 Da, PEG600), triphenylphosphine, thioctic acid, 4-(*N*,*N*-dimethylamino)pyridine, triethylamine, and *N*,*N*′-dicyclohexylcarbodiimide were purchased from

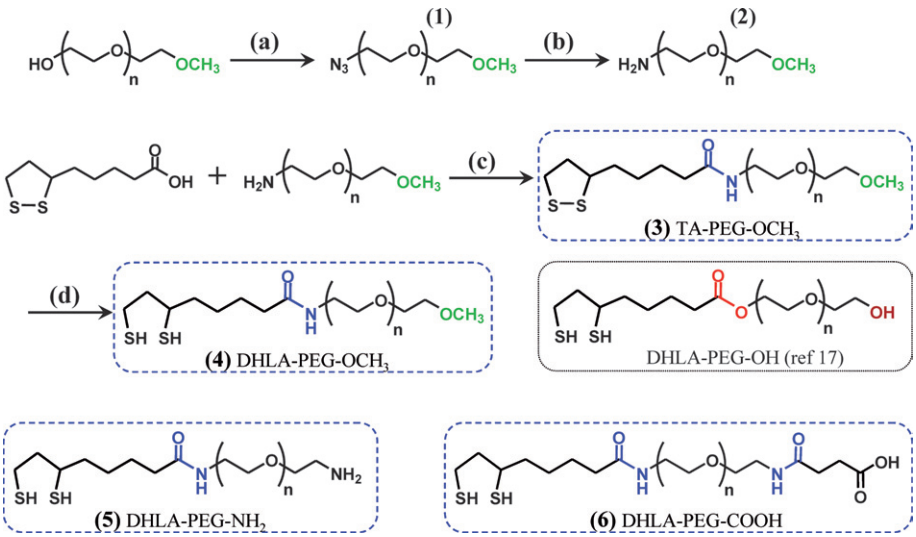

Fig. 1 Chemical structures and synthetic scheme of ligands described in this study. Reactions used: (top) (a) (i) CH_3SO_2Cl, Et_3N, THF; (ii) H_2O, NaN_3, $NaHCO_3$, (b) PPh_3, H_2O, THF, (c) DCC, DMAP, CH_2Cl_2, (d) $NaBH_4$, MeOH, H_2O. Note the new methoxy terminal group and the amide bond in the final products in comparison to DHLA-PEG-OH reported in ref. 17. The ester bond highlighted in red is labile during reduction of the 1,2 dithiolane. Ligands **5** and **6**, DHLA-PEG600 ligands with amine and carboxyl terminal groups, respectively, are also illustrated (bottom).

Acros Organics (Morris Plains, NJ). Poly(ethylene glycol) methyl ether (mPEG, average molecular weights 550 and 750 Da), reagent grade celite, thin layer column chromatography (TLC) plates (silica gel matrix with aluminium support) and all solvents were purchased from Sigma Aldrich. Sodium azide was purchased from Alfa Aesar (Ward Hill, MA). Methanesulfonyl chloride was purchased from GFS Chemicals (Powell, OH). Sodium borohydride ($NaBH_4$) was purchased from Strem Chemicals (Newburyport, MA). Citrate-stabilized colloidal gold (15 nm in diameter) solutions were purchased from Ted Pella, Inc. (Reading, CA). Low-EEO agarose and 10× Tris borate EDTA buffer were purchased from Fisher Scientific. Tetrahydrofuran (THF) was dried over basic alumina before use. Column chromatography was performed using silica gel (Bodman Industries, Aston, PA; 60 Å, 230–400 mesh). Deuterated chloroform ($CDCl_3$) for NMR measurements was used as received.

^{1}H NMR spectra were recorded on a Bruker SpectroSpin 400 MHz spectrometer, and chemical shifts for ^{1}H NMR spectra were reported relative to tetramethylsilane (TMS) signal in the deuterated solvent (TMS, $\delta = 0.00$ ppm). All J values are reported in Hertz. Fourier transform infrared (FT-IR) spectra were measured on a Nicolet Nexus 870 FT-IR spectrometer (Thermo Fisher Scientific, Inc., Waltham, MA). UV-Vis absorption spectra were collected using an HP 8453 diode array spectrophotometer (Agilent technologies, Santa Clara, CA), while the fluorescence spectra were collected using a Spex Fluorolog-3 spectrophotometer (Jobin Yvon Inc, Edison, NJ) equipped with a red-sensitive R2658 Hamamatsu PMT detector.

2. Synthesis and design

The synthesis of DHLA-PEG-OCH_3 ligands used for cap exchange with the nanocrystals can be summarized in four main reaction steps: (1) azide transformation of the hydroxy group at the end of mPEG using methanesulfonyl chloride and sodium azide, (2) transformation of the azide group to an amine by reduction with triphenylphosphine, (3) coupling of the amine on the mPEG to TA, *via* *N*,*N*′-dicyclohexylcarbodiimide (DCC) coupling to make TA-PEG-OCH_3 and (4) ring opening of the 1,2-dithiolane end group (*via* sodium borohydride reduction) to make the final DHLA-PEG-OCH_3 ligand. The synthetic scheme described below equally applies to the preparation of ligands having various PEG molecular weights. In the present study, details of the synthesis, purification and use for nanoparticle functionalization will be limited to ligands having mPEG average molecular weights of 550 and 750 Da. We will refer to ligands having PEG750 throughout the manuscript, unless otherwise stated. We also synthesized DHLA-PEG ligands that have amine and carboxyl terminal groups using PEG600.

Synthesis of N_3-PEG750-OCH_3 (1). Poly(ethylene glycol) methyl ether (MW ~ 750 Da) (60.0 g, ~8.0×10^{-2} mol) and methanesulfonyl chloride (11.95 g, 0.104 mol) were first dissolved in 100 mL of THF in a 500 mL round-bottom flask and the solution was cooled to ~0 °C under N_2 using an ice-bath. Triethylamine (16.2 mL, 0.12 mol) was added dropwise to the reaction flask using an addition funnel. The reaction mixture was then gradually warmed to room temperature and left stirring overnight. To this mixture, a solution of $NaHCO_3$ (7.0 g, 8.33×10^{-2} mol) in 125 mL of H_2O was added, followed by sodium azide (8.33 g, 0.128 mol) while stirring. The content was then heated to distill off the THF and refluxed for 7 h. After cooling, the reaction mixture was extracted three times with ethyl acetate. The combined organic layers were dried over Na_2SO_4, filtered and the solvent was evaporated to obtain the product (~75% yield). The product was a waxy solid at room temperature. TLC of the product was carried out using a 10 : 1 (v/v) CH_2Cl_2 : methanol (MeOH) eluent resulting in $R_f \sim 0.53$. ^{1}H NMR (400 MHz, in $CDCl_3$): δ 3.62–3.71 (m), 3.53–3.57 (m, 2H), 3.39 (t, 2H, $J = 5.2$ Hz), 3.38 (s, 3H).

Synthesis of NH_2-PEG750-OCH_3 (2). N_3-PEG750-OCH_3 (46.5 g, ~6.0×10^{-2} mol) and triphenylphosphine (21.9 g, 8.35×10^{-2} mol) were mixed in a 500 mL round-bottom flask, dissolved in 400 mL THF and left to stir for 30 min. Then, H_2O (10 mL, 0.54 mol) was added and the solution further stirred for 4 h under N_2 at room temperature. The THF was evaporated and 400 mL of a 1 M HCl solution was added to the mixture. The reaction mixture was then extracted with ethyl acetate (3 times), which allowed removal of a fast moving by-product as shown by TLC. The reaction mixture was basified by saturating with $NaHCO_3$, then with NaCl, and extracted with CH_2Cl_2. The organic layers were combined and dried over Na_2SO_4, filtered, and evaporated to obtain the product (~97% yield), which was a waxy solid at room temperature. TLC of the product using a 5 : 1 (v/v) CH_2Cl_2 : MeOH eluent resulted in $R_f \sim 0.47$. ^{1}H NMR (400 MHz, in $CDCl_3$): δ 3.62–3.71 (m), 3.53–3.57 (m, 2H), 3.51(t, 2H, $J = 5.2$ Hz), 3.38 (s, 3H), 2.87 (t, 2H, $J = 5.2$ Hz).

Synthesis of TA-PEG750-OCH_3 (3). NH_2-PEG750-OCH_3 (32.8 g, ~4.46×10^{-2} mol), 4-(*N*,*N*-dimethylamino)pyridine (1.10 g, 9.0×10^{-3} mol), *N*,*N*′-dicyclohexylcarbodiimide (9.26 g, 4.49 $\times 10^{-2}$ mol) and 150 mL of CH_2Cl_2 were mixed in a 500 mL round-bottom flask. The content was stirred under N_2 and cooled to 0 °C using an ice-bath. Thioctic acid (9.20 g, 4.46×10^{-2} mol), dissolved in 50 mL of CH_2Cl_2, was slowly dripped into the reaction using an addition funnel. The reaction mixture was left stirring for 2 h at 0 °C, then slowly warmed to room temperature and left to stir overnight under N_2. The mixture was filtered through celite, rinsed with ethyl acetate, and the solvent was evaporated from the filtrate. After evaporating the solvent, the reaction mixture was diluted with 200 mL of H_2O and extracted with ether to remove a fast moving by-product as shown by TLC. Then the aqueous solution was saturated with $NaHCO_3$ and the crude product was extracted with CH_2Cl_2. The combined extracted CH_2Cl_2 layers were dried over Na_2SO_4, filtered and the solvent was evaporated. The crude product was chromatographed on silica gel with 10 : 1 (v/v) CH_2Cl_2 : MeOH as the eluent to obtain the product (~70% yield), which was a yellow waxy solid at room temperature. TLC of the product using a 10 : 1(v/v) CH_2Cl_2 : MeOH eluent resulted in $R_f \sim 0.46$. ^{1}H NMR (400 MHz, in $CDCl_3$): δ 6.29 (br s, 1H), 3.62–3.71 (m), 3.53–3.57 (m, 4H), 3.46 (t, 2H, $J = 5.2$ Hz), 3.38 (br s, 3H), 3.08–3.22 (m, 2H), 2.42–2.52 (m, 1H), 2.19 (t, 2H, $J = 7.2$ Hz), 1.86–1.96 (m, 1H), 1.59–1.78 (m, 4H), 1.40–1.55 (m, 2H).

Synthesis of DHLA-PEG750-OCH_3 (4). TA-PEG750-OCH_3 (0.33 g, 3.46×10^{-4} mol) was dispersed in a mixture of 1 mL of

MeOH and 2 mL of H_2O; the container was sealed, purged with N_2 and cooled to ~0 °C using an ice-bath. $NaBH_4$ (2.7×10^{-2} g, 7.14×10^{-4} mol) dissolved in 2 mL of H_2O was slowly injected into the reaction mixture, and the solution was left stirring for an additional 2 h at 0 °C. The reaction mixture was then warmed to room temperature and left to stir overnight. The content was diluted with 15 mL of brine, and extracted with CH_2Cl_2. The combined organic phase was dried over Na_2SO_4, filtered and the solvent evaporated to obtain the product (a yield of ~97%), as a white waxy solid at room temperature. TLC of the reduced ligand (DHLA-PEG750-OCH_3) co-spotted with TA-PEG750-OCH_3 and eluted using 10 : 1 (v/v) CH_2Cl_2 : MeOH showed similar positions, but DHLA-PEG750-OCH_3 exhibited a band with a longer tail. ^{1}H NMR (400 MHz, in $CDCl_3$): δ 6.29 (br s, 1H), 3.62–3.71 (m), 3.53–3.57 (m, 4H), 3.46 (t, 2H, $J = 5.2$ Hz), 3.38 (s, 3H), 2.92 (m, 1H), 2.6–2.8 (m, 2H), 2.20 (t, 2H, $J = 7.2$ Hz), 1.85–1.95 (m, 1H), 1.40–1.80 (m, 7H), 1.36 (t, 1H, $J = 8.0$ Hz), 1.31 (d, 1H, $J = 7.6$ Hz).

Synthesis of DHLA-PEG600-NH_2 (5) and DHLA-PEG600-COOH (6). These ligands were synthesized using a similar procedure as reported in reference 18, with a few necessary changes made as a result of the longer PEG chain (PEG400 was used in ref. 18). The most important improvement pertained to the synthesis of NH_2-PEG600-N_3, which is the intermediate required for DCC coupling to TA. The detailed synthetic procedure of all the intermediates and final compounds is provided in the ESI.†

3. Quantum dot synthesis and cap exchange

QDs used in this study were CdSe–ZnS core–shell nanocrystals synthesized stepwise in our laboratory using high temperature reaction of organometallic precursors (*e.g.*, trioctylphosphine selenium (TOP : Se), cadmium acetylacetonate, diethylzinc and hexamethyldisilathiane) in a hot coordinating mixture of TOP/TOPO and hexadecylamine, as described in the literature.[13–16] Cap exchange of the TOP/TOPO-capped QDs with neat DHLA-PEG750-OCH_3 or a mixture of DHLA-PEG750-OCH_3 and amine-terminated or carboxyl-terminated DHLA-PEG (DHLA-PEG600-NH_2 or DHLA-PEG600-COOH, respectively) was carried out following the procedure we previously detailed.[17,18] In a typical cap exchange preparation, ~0.5 mL of as-prepared hydrophobic QDs dispersed in a mixture of hexane–toluene–butanol (~20–40 μM in QD concentration) was first precipitated by adding ~10 mL of ethanol. The mixture was then centrifuged and the supernatant decanted. 5 mL of ethanol were added to the precipitate and the mixture was briefly sonicated to break up the pellet. The dispersion was centrifuged again, and the supernatant decanted. 0.5 mL (~5×10^{-4} mol) of the ligand was added to the precipitated QDs, and the vial was sealed and purged with N_2. In general a large excess of ligands (25000–50000 ligands per QD) is used to allow effective cap exchange, because the process is driven by mass action. Ethanol (0.5 mL) was then injected *via* a syringe into the vial, and the mixture was stirred for several hours at 60–80 °C. As the sample homogenized, it became clear, which is indicative of effective cap exchange. The solution was cooled to room temperature and then precipitated with a mixture of hexane, ethanol, and CH_2Cl_2 (roughly in a mixing ratio of 1.0 : 1.2 : 0.1). The sample was then centrifuged; the supernatant discarded and residual solvents were evaporated over flowing N_2. The relatively dry and newly capped QDs were re-dispersed in deionized water to form a clear dispersion of nanoparticles. The dispersion was subsequently filtered through a 0.45 μm hydrophilic membrane (Millipore). Excess free solubilized ligands were removed from the final dispersion by exchanging the solvent with fresh DI water 2–3 times (~15 mL per cycle) using a centrifugal filtration device (Millipore, MW cutoff of 50 kDa). The cap-exchanged QDs were characterized using absorption, fluorescence, and FT-IR spectroscopy. The QD concentrations were determined from UV-Vis absorption measurements following the procedure reported by Leatherdale *et al.*[28]

4. Ligand cap exchange on gold nanoparticles

Cap exchange of gold nanoparticles (AuNPs) with the new ligands was performed on commercially available citrate-stabilized colloidal gold solutions (Ted Pella, Inc., Reading, CA).[29] We also found that both 1,2-dithiolane- and dithiol-terminated ligands provided effective cap exchange with AuNPs, a clearly different result from what we have observed for QDs; for the latter, ring opening of the 1,2-dithiolane is required. TA-PEG-OCH_3 or DHLA-PEG-OCH_3 was diluted in 1 mL of DI water (35 mg, ~3.7×10^{-5} mol) and the solution pH was adjusted to 10 by adding a drop of 0.5 M NaOH. The ligand solution was added to citrate-stabilized AuNPs (4 mL, ~1.4×10^{12} particles mL^{-1}) and the dispersion stirred overnight (~18 h) at room temperature. For cap exchange on AuNPs we used an excess of 4×10^6 ligands per nanocrystal, which corresponds to 400 ligands per surface atom, assuming that a 15 nm AuNP has ~10 000 surface atoms.[7] The mixture was then filtered through a 0.45 μm hydrophilic membrane, and excess ligand was removed by washing with water (2–3 times, ~15 mL each cycle) using a centrifugal filtration device (Millipore, MW cutoff of 50 kDa), as described above. The cap-exchanged AuNPs were characterized by FT-IR and absorption spectroscopy. The extinction coefficient of the 15 nm AuNPs (as-received concentration of ~1.4×10^{12} particles mL^{-1}) was determined to be ~4.2×10^8 M^{-1} cm^{-1} at their plasmon peak of 524 nm. The measured extinction coefficient is consistent with literature values and was used to determine the concentration of the AuNPs after cap exchange.[30,31]

5. pH Stability of cap-exchanged nanoparticles

After cap exchange, the stability of the nanoparticles (QDs and AuNPs) in both acidic and basic conditions was monitored over time. For comparison, commercially purchased polymer coated carboxyl QDs (Invitrogen, CA) were also tested. As provided these QDs are stored in 50 mM borate buffer, which was exchanged with DI water using a centrifugal filtration device (Millipore, MW cutoff of 50 kDa). Buffers of varying pH were prepared by adding 2 M HCl or NaOH to 1× phosphate buffered saline (PBS). The samples were monitored over time and photographs were taken at various time intervals under UV or white light illumination for QDs and AuNPs, respectively.

6. Gel electrophoresis

Gel electrophoresis experiments were conducted using QDs that were cap-exchanged with either a homogeneous (using one type of ligand) or a heterogeneous surface cap (using mixtures of either DHLA-PEG-OCH_3 and DHLA-PEG600-NH_2 or DHLA-PEG-OCH_3 and DHLA-PEG600-COOH). The nanocrystal dispersions were run on 1% agarose gel using tris borate EDTA buffer (TBE, 89 mM tris borate, 2 mM EDTA) that was adjusted to pH 6.9 by adding diluted HCl. QD samples were diluted to ~1–2 μM concentrations in a 10% glycerol TBE–HCl loading buffer immediately prior to use. The experiments were conducted using a voltage of 3–5 V cm^{-1} and fluorescence images were captured using a Kodak 440 Digital Image Station.

7. Live cell injection and imaging with cap-exchanged quantum dots

COS-1 cell lines (ATCC, Manassas, VA) were cultured following the procedures previously described.[32] Microinjection was performed in sterile Lab-Tek chambered coverslips (Nunc, Rochester, NY). The chambers were coated with 50 μg mL^{-1} fibronectin (Sigma-Aldrich) in sodium bicarbonate buffer pH 8.5, and ~2×10^4 cells were seeded into the wells and cultured overnight. DHLA-PEG750-OCH_3 and DHLA-PEG600-OH capped QDs (5 μM concentration, in 0.5× PBS) were directly injected into adherent cells using an InjectMan® NI2 micromanipulator equipped with a FemtoJet Programmable Microinjector (Eppendorf, Westbury, NY). This setup allows the injection of femtoliter aliquots of conjugate solution to individual cells. The cell cultures were subsequently imaged using an Olympus IX-70 microscope (Center Valley, PA). Cultures were excited using 488 nm light provided by a Xe lamp source combined with a 488 nm band pass filter (Chroma Technology, Rockingham, VT). The fluorescence emission was separated from the excitation signal using a 500 nm long-pass filter (Chroma Technology, Rockingham, VT) and collected on a DP71 color digital camera (Olympus, Center Valley, PA). Differential interference contrast (DIC) images of the cell cultures were also collected on the same Olympus IX-70 microscope using a bright field source. The images were then analyzed using DP Manager Software (Olympus, Center Valley, PA) and Image J (NIH, Bethesda, MD). After injections, the cells were incubated at 37 °C in Ringer's solution and were periodically taken out to ambient conditions for microscopy imaging.

Results and discussion

Synthesis and characterization

The synthetic scheme and chemical structures of the ligands made and used for cap exchange are illustrated in Fig. 1. The synthetic design essentially follows our previously published rationale.[18] The terminal hydroxy group on the poly(ethylene glycol) methyl ether (mPEG) was first converted to an azide *via* a two-step reaction. The first consisted of converting the hydroxy to a methanesulfonyl intermediate group and then to an azide by sodium azide (step a). In the second, the azide group was transformed to an amine using triphenylphosphine (step b), followed by attachment to thioctic acid (TA) *via* DCC coupling to provide TA-PEG-OCH_3 (step c). Finally, the 1,2-dithiolane ring on the TA unit was reduced with $NaBH_4$ (step d). In reaction steps a, b and d, the solubility of the resulting molecules was taken into careful consideration and the products were purified by extraction, rather than column chromatography, an approach that has greatly simplified the overall synthetic scheme.

We should also emphasize that because the mPEG precursor presents only one reactive end group, the synthesis of the amino-PEG (NH_2-PEG-OCH_3) was carried out without requiring a biphasic reaction as done previously.[18,33] Using mPEG not only simplified this synthetic step, but the yield was also dramatically increased to values exceeding 90%; we reported a yield of ~50% for the NH_2-PEG-N_3 reaction in reference 18. In addition, only ~1 : 1 molar ratio of PEG to TA was used for the present coupling scheme. This constitutes a major improvement compared to the esterification reaction we reported in reference 17, where a 10-fold molar excess of PEG was used in order to suppress the formation of bis-substituted PEG (TA-PEG-TA). These two advantages make the synthesis route more efficient than previously reported.

One of the key features of the TA-PEG-OCH_3 ligand (**3**) is the presence of an amide bond, instead of an ester, which leads to improved ligand stability. For example, we found that reduction of ligand **3** in the presence of even a 3–4 fold excess $NaBH_4$ did not affect the coupling integrity, whereas even an equimolar ratio of $NaBH_4$ to TA-PEG-OH occasionally induces decomposition of the molecule, most likely a consequence of the labile nature of the ester bond. The ^{1}H NMR data shown in Fig. 2 clearly prove that the spectrum of compound **3** is a composite of the individual spectra collected for the two precursors (mPEG and TA), with a very pronounced peak at 3.6–3.7 ppm characteristic of the PEG segment, a singlet peak at 3.38 ppm attributed to the methoxy group, and a new broad singlet peak at ~6.3 ppm attributed to the amide proton.[17,18] Following ring opening, the ^{1}H NMR spectrum of DHLA-PEG-OCH_3 (**4**) shows additional triplet and doublet peaks at ~1.3–1.4 ppm, which are attributed to the open dithiol protons (Fig. 2). In addition to the amide proton peak at ~6.3 ppm, the triplet peak attributed to the protons from the PEG segment closest to the amide bond (3.46 ppm) and the triplet from the protons next to the carbonyl (2.20 ppm) were also observed in compound **4**. This confirms

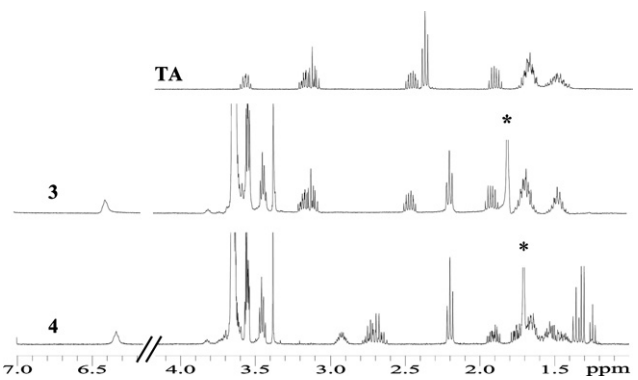

Fig. 2 ^{1}H NMR spectra of thioctic acid (TA), **3** (TA-PEG750-OCH_3) and **4** (DHLA-PEG750-OCH_3) measured in $CDCl_3$. The large peak in the spectra at ~1.6 ppm, marked by *, is attributed to water.

that the integrity of the coupling *via* the amide bond was maintained even when the 1,2-dithiolane reduction was carried out using a 3-fold excess of $NaBH_4$.

The synthesis of DHLA-PEG600-NH_2 (**5**) and DHLA-PEG600-COOH (**6**) was an extension of our previous approach for preparing amine-, carboxyl- and biotin-functionalized DHLA-PEG ligands. In reference 18, all bifunctional ligands were prepared using PEG400 chain, due to a combination of ease of implementation and purification. Extension of the synthesis scheme to ligands with a PEG600 chain required retooling of the synthetic steps and led to improved purification techniques. The major and most relevant change pertained to the synthesis and purification of N_3-PEG600-NH_2. In particular, replacing the ether (used for PEG400) with ethyl acetate in the biphasic medium is important, as the latter offers better control over the solubility of the larger PEG segment and the overall reaction efficiency.[34] Purification of N_3-PEG600-NH_2 was also simplified and made more efficient by replacing silica gel chromatography with a simple liquid–liquid extraction. These improvements culminated in the increase of the reaction yield from ~50% to values exceeding 70%. This is very important since this compound is a required precursor for synthesizing all the other end-functionalized TA- and DHLA-PEG ligands (namely **5** and **6** shown in Fig. 1).

Ligand exchange on semiconducting and gold nanoparticles

The new sets of ligands were used to functionalize the surface of luminescent QDs as well as AuNPs. Nonetheless, the schemes developed slightly varied from one set of materials to the other.

a. Cap exchange on luminescent QDs. Cap exchange of the native TOP/TOPO ligands with DHLA-PEG750-OCH_3 (**4**) neat or mixed with either DHLA-PEG600-NH_2 (**5**) or DHLA-PEG600-COOH (**6**) was effective in promoting the transfer of the nanocrystals to buffer solutions at both acidic and basic pHs. Following transfer the QDs maintained their absorption and luminescence characteristics, as shown in Fig. 3 for a typical QD sample emitting at 552 nm and cap-exchanged with DHLA-PEG750-OCH_3 (**4**); spectra of TOP/TOPO-coated QDs (control) dispersed in CH_2Cl_2 are shown for comparison. However, a reduction of the PL quantum yield compared to the TOP/TOPO-capped samples was observed. In general the quantum yield experiences about 50% reduction compared to TOP/TOPO-capped nanocrystals dispersed in hexane or toluene, a result that is consistent with our previous findings using the DHLA-PEG-OH cap.[17,18] Cap exchange with DHLA-PEG550-OCH_3 (PEG MW ~ 550 Da) also promotes water solubility of luminescent QDs as shown in Fig. S1 (ESI†). This indicates that the PEG segment dominates the solubility of the QD ligand in aqueous environments since both the dihydrolipoic acid and methoxy groups are hydrophobic.

b. Ligand exchange on gold nanoparticles. To extend the utility of our ligand design we performed cap exchange on commercially available citrate-functionalized AuNPs (Ted Pella, Inc., Reading, CA). Cap exchange was carried out successfully using both TA-PEG-OCH_3 (**3**) and DHLA-PEG-OCH_3 (**4**). Fig. 4 shows the absorption spectra of solutions of 15 nm AuNPs before and after cap exchange with either of the ligands. The data clearly indicate that substituting the citrate with either of the two ligands did not affect the native properties of the nanoparticles, with essentially no change in the absorption features and absence of any aggregate formation following the surface modification. The effective cap exchange of AuNPs using TA-PEG as well as DHLA-PEG ligands is attributed to the strong affinity of the dithiol end group (soft base) to the gold surface (soft acid).[7,35–37] The ability to perform cap exchange of metallic nanoparticles using 1,2-dithiolane without ring opening is potentially advantageous, because it reduces the number of reaction steps needed while still benefiting from the stronger bidentate coordination (compared with single thiol) to the nanoparticle surface. This is drastically different from cap exchange of QDs, where opening of the dithiolane ring is always required.

To further verify the effectiveness of the cap exchange on AuNPs, we compared the stability of the citrate-functionalized

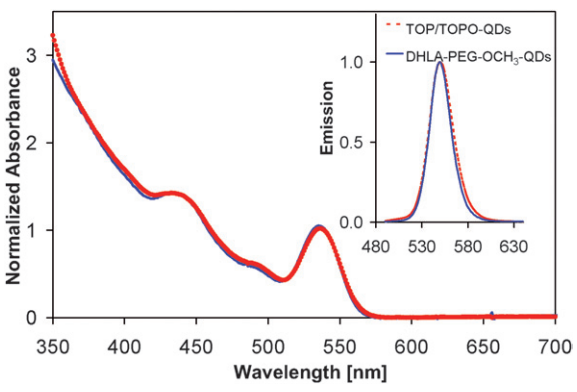

Fig. 3 Absorption spectra of as-prepared QDs capped with TOP/TOPO in CH_2Cl_2 (red, dotted line) and QDs that were cap-exchanged with DHLA-PEG750-OCH_3 (blue, solid line). The two spectra are normalized to the first exciton peak. Inset: Normalized fluorescence spectra of as-prepared QDs and QDs cap-exchanged with DHLA-PEG-OCH_3. The QD concentration used in these experiments was ~100 nM.

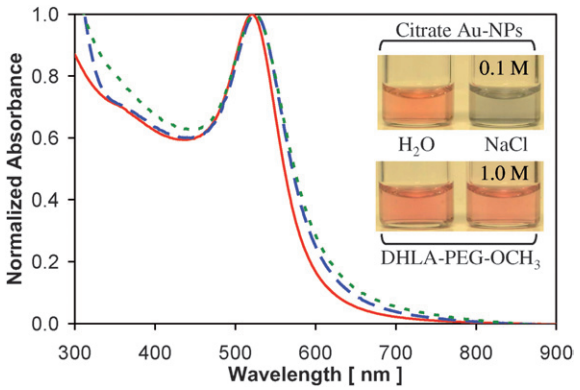

Fig. 4 Absorption spectra of as-purchased AuNPs stabilized with citric acid (red, solid line), cap-exchanged with TA-PEG-OCH_3 (green, dotted line), and DHLA-PEG-OCH_3 (blue, dashed line). The spectra are normalized to the first plasmon peak. Inset: Images of citrate-stabilized AuNPs in H_2O and 30 minutes after addition of 0.1 M NaCl (top), DHLA-PEG-OCH_3-capped AuNPs in H_2O and 1.0 M of NaCl (bottom). The nanoparticle concentration is ~1.5 pM.

and DHLA-PEG-OCH_3-capped AuNPs in the presence of excess electrolyte (*i.e.*, NaCl). Although the as-received citrate-functionalized nanoparticles were stable at low counter-ion excess, we found that when NaCl concentration was increased (to ~100 mM) the AuNPs readily precipitated (see inset in Fig. 4). In comparison, we found that after cap exchange with TA-PEG-OCH_3 or DHLA-PEG-OCH_3, dispersions of AuNPs were stable and aggregate-free at concentrations exceeding 1 M NaCl (see inset in Fig. 4). Additional stability tests indicate that the newly capped AuNPs are stable and aggregate-free for at least several months in 1 M NaCl. This demonstrates the ability of the TA- and DHLA-based PEG ligands to effectively cap the AuNPs and improve their thermodynamic stability, even in the presence of high concentrations of excess counter-ion.

c. FT-IR of cap-exchanged nanoparticles. FT-IR measurements, shown in Fig. 5, were performed on QDs and AuNPs before and after cap exchange to confirm that the surface ligands were indeed attached to the nanoparticles. The data show that spectra collected for the solution of cap-exchanged QDs and AuNPs are similar to those of the free ligand (*i.e.* they exhibit all the same major bands). Most notably, the spectra of cap-exchanged nanoparticles exhibit sharp bands at 1670 cm^{-1} and 1540 cm^{-1}, which are attributed to the amide I (C═O stretch) and amide II (N–H bending) from the bond linking the TA to mPEG, as does the free ligand spectrum. These two distinct bands are, however, not present in the spectra of TOP/TOPO-QDs or citrate-stabilized AuNPs. Furthermore, the large band at 1590 cm^{-1} (C═O stretch from citrate) measured on the citrate-stabilized AuNPs was not present in the cap exchanged AuNPs. These data suggest that effective cap exchange of both QDs and AuNPs using the newly synthesized DHLA-PEG-OCH_3 ligands has indeed taken place.

d. pH Stability of nanoparticles. The stability of QDs and AuNPs capped with the mPEG-appended DHLA and TA ligands was also tested under various pH conditions. For comparison, the pH effects on commercially available polymer-encapsulated nanocrystals were also studied. Fig. 6A shows the fluorescence of several solutions of green-emitting QDs cap-exchanged with DHLA-PEG-OCH_3 dispersed in 1× PBS over the pH range 3–13. The images show that the dispersions are stable for over one week; at pH levels between 4 and 11, these solutions are stable for at least one month. These findings confirm and expand our previous stability results using OH-terminated ligands; DHLA-PEG600-OH-QDs were stable over a narrower pH range (5–10).[17,18] Similar experiments performed on polymer-encapsulated QDs (Invitrogen) showed that dispersions of these nanocrystals are stable only at neutral to

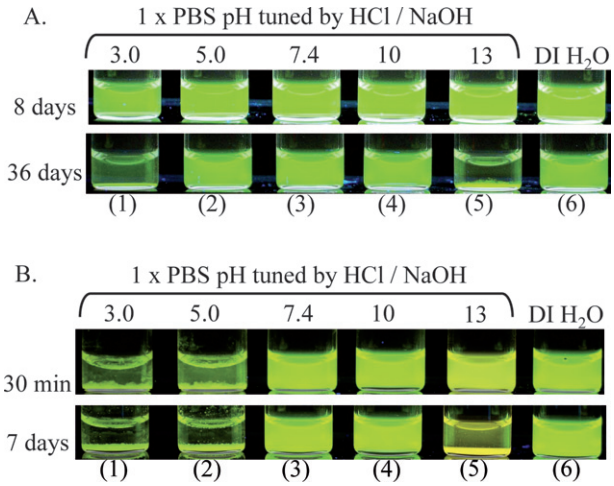

Fig. 6 (A) Luminescence images of DHLA-PEG-OCH_3 cap-exchanged CdSe-ZnS QDs (λ_{em} = 552 nm) in PBS at varying pH after 8 days and 36 days of storage at 4 °C. Vial 6, containing CdSe-ZnS diluted with DI water, serves as a control sample. (B) Luminescence images of commercially available carboxylated CdSe-ZnS QDs (λ_{em} = 565 nm) in 1× PBS at varying pH after 30 min and 7 days of storage at 4 °C. Vial 6, containing as-received QDs (in 50 mM borate) diluted with DI water, serves as a control sample. Samples were excited with a hand-held UV lamp at 365nm, and had ~0.5 μM concentration.

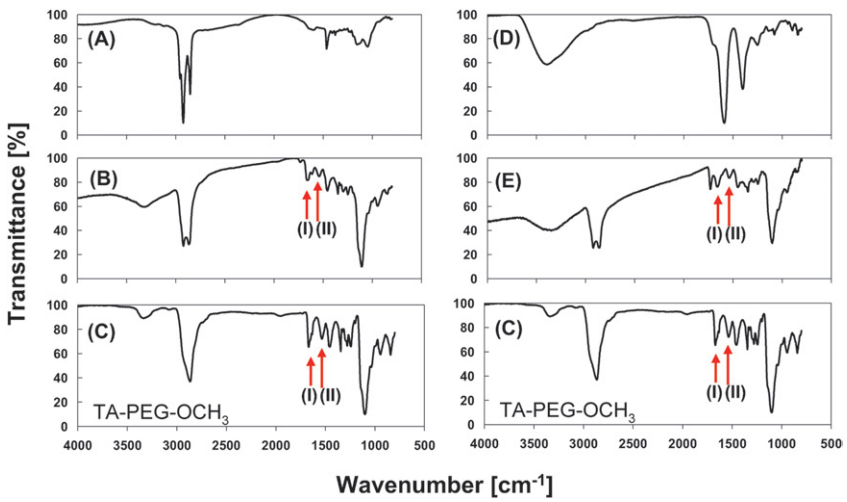

Fig. 5 FT-IR spectra of (A) TOP/TOPO-QDs, (B) DHLA-PEG-OCH_3-QDs, (C) TA-PEG-OCH_3 ligands (shown twice for easy cross-reference), (D) as-purchased citrate stabilized AuNPs, (E) TA-PEG-OCH_3-AuNPs. The arrows indicated the bands attributed to amide I and II, which originate from the amide bond that links TA to mPEG.

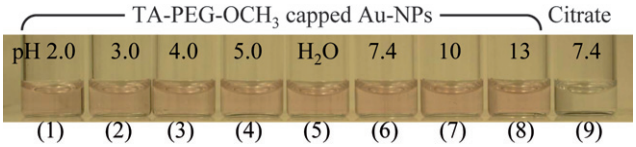

Fig. 7 Image of AuNPs in PBS of varying pH after 3 weeks at room temperature. Vials 1–4 and 6–8 contain AuNPs capped with TA-PEG-OCH_3 in pH 2.0, 3.0, 4.0, 5.0, 7.4, 10, and 13, respectively. Vial 5, containing AuNPs capped with TA-PEG-OCH_3 in DI water, serves as a control sample. Vial 9 contains citrate-stabilized AuNPs in 1× PBS (pH 7.4). The nanoparticle concentration is ~0.5 pM.

basic buffer conditions. The nanocrystals aggregate immediately following transfer to PBS buffers under acidic conditions, as shown in Fig. 6B. At pH 13, the nanocrystals also exhibit a red shift of the photoluminescence shortly after transfer into the buffer and macroscopic aggregation after 1 week. We should emphasize that the QDs stay luminescent throughout the experiments. At unfavourable pH, small aggregates slowly grow with time and settle at the bottom of the vial.

Dispersions of DHLA-PEG-OCH_3-AuNPs in PBS buffers were stable over the pH range 2–13 for at least three months, as shown in Fig. 7. The stability of QDs and AuNPs capped with the new set of ligands offers a great deal of flexibility for using these hydrophilic nanoparticles for biological experiments, where harsh conditions are ubiquitous. For example, many cellular organelles are maintained at acidic conditions and rich in dissolved ions.

Gel electrophoresis of cap-exchanged quantum dots

One of the key properties of the hydrophilic QDs prepared using the current ligand design is the ability to potentially control the nature and fraction of functional groups on the nanocrystal surface, simply achieved *via* mixed surface cap exchange. We verified this property by monitoring, on the same gel, changes in the electrophoretic mobility of QD dispersions capped with mixtures of either DHLA-PEG-OCH_3 and DHLA-PEG600-NH_2 or DHLA-PEG-OCH_3 and DHLA-PEG600-COOH. The molar ratios of the end-functionalized ligand (NH_2 or COOH) in the mixtures were also varied. Fig. 8 shows a comparison of the mobility shift of 552 nm emitting QDs cap-exchanged with different ligand compositions after 15 min of electrophoresis: DHLA-PEG600-COOH : DHLA-PEG-OCH_3 at molar fractions of carboxyl groups between 5% and 30% (lanes 1–3); neat DHLA-PEG-OCH_3 (lane 4); and DHLA-PEG-OCH_3 : DHLA-PEG600-NH_2 with molar fractions of amines between 5% and 60% (lanes 5–8). No QD migration was measured for nanocrystals capped with neat DHLA-PEG750-OCH_3 (lane 4), indicating that these QDs were essentially neutral. In contrast, QDs having a small fraction of DHLA-PEG600-COOH ligand migrated towards the positive electrode, while QDs surface-modified with a fraction of DHLA-PEG600-NH_2 ligand migrated towards the negative electrode, as anticipated from the nature of the end groups. Furthermore, the mobility shift depended on the fraction of charged ligands used for the cap exchange, with larger shifts measured for larger molar ratios. The changes in mobility shifts measured for the various samples were

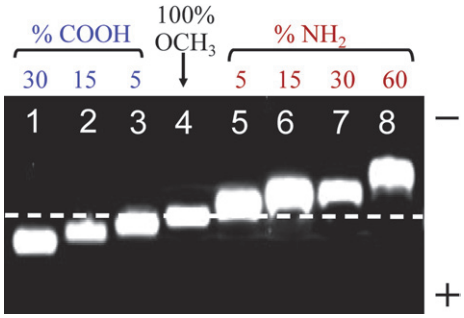

Fig. 8 Gel electrophoresis images of QDs capped with different surface ligands: (1) 30% COOH : 70% OCH_3, (2) 15% COOH : 85% OCH_3, (3) 5% COOH : 95% OCH_3, (4) 100% OCH_3, (5) 5% NH_2 : 95% OCH_3, (6) 15% NH_2 : 85% OCH_3, (7) 30% NH_2 : 70% OCH_3, (8) 60% NH_2 : 40% OCH_3. Dashed line indicates the location of the wells.

consistent with the nature and percentage of the chargeable units present at the end of the ligands. It is important to note that the proposed surface capping strategy has a few unique advantages. (1) Since all the ligands are designed to have the same anchoring group, the same cap exchange method can be used with any mixture of such ligands to produce QDs and AuNPs with the desired heterogeneous surface functionalities. (2) Control over the density of a specific function can be achieved by mixing the corresponding ligand with the inert DHLA-PEG750-OCH_3. This provides the means to precisely control the fraction of added chemical functionalities on the nanocrystal surface.

Live cell imaging

In previous work, we have shown that appending a PEG-hydroxy segment onto DHLA could improve the stability of luminescent DHLA-PEG600-OH-QDs in acidic buffers and QDs microinjected into the cytoplasm of HeLa cells, particularly when compared to DHLA-QDs.[17] The terminal hydroxy group on DHLA-PEG600-OH we used in references 17 and 18 is still reactive (*e.g.* isocyanate[24] or *via* DCC coupling). To test whether the presence of the methoxy terminal group could provide additional advantages to the new ligands compared to DHLA-PEG600-OH in intracellular studies, we microinjected live COS-1 cells with QDs capped with either DHLA-PEG600-OH or DHLA-PEG750-OCH_3 and followed the fluorescence distribution in the cells up to 32 h post injection.[25] Representative fluorescence images, shown in Fig. 9, indicate that cells microinjected with either QDs exhibit strong emission from the QDs after 32 h of incubation in Ringer's solution. The slow decrease of the detected signal is attributed to the ion-rich medium used for cell culturing; we have previously observed that the fluorescence of QDs persists in buffers and DI water over extended periods of time under continuous illumination.[38] Images show that the nanocrystal distribution remains perinuclear for both sets of surface-functionalized QDs. They also show that punctuate fluorescence patterns progressively develop in the cells microinjected with DHLA-PEG600-OH-QDs over the experimental time frame, a result similar to our earlier observation using HeLa cells in reference 17. In comparison, the fluorescence pattern for DHLA-PEG-OCH_3-QDs is more homogeneous throughout the 32 h "incubation" time. Additional cell micrographs (DIC and

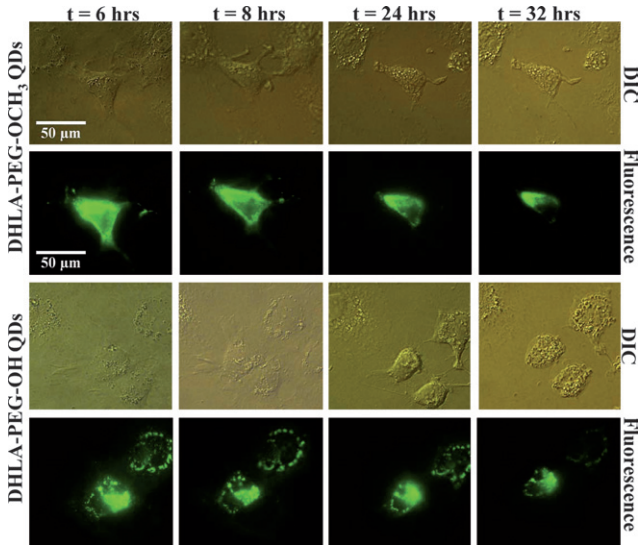

Fig. 9 Micrographs of COS-1 cells injected with 552 nm emitting QDs capped with DHLA-PEG750-OCH_3 (top) and DHLA-PEG600-OH (bottom) and monitored for 32 h after microinjection. Following microinjection, cells were stored at 37 °C in Ringer's solution.

fluorescence) are shown in ESI† (Fig. S2). These preliminary results are promising. They clearly indicate that improved intracellular stability and reduced levels of non-specific interactions characterize QDs capped with the methoxy-terminated ligands (DHLA-PEG-OCH_3-QDs) compared with those functionalized with ligands that have an ester linkage and present OH terminal groups (DHLA-PEG-OH-QDs). This also leads us to anticipate that in addition to the difference between the amide and ester bonds, the terminal groups presented on the nanoparticles play an important role in promoting or reducing non-specific interactions, particularly in ion-rich growth media and inside live cells. Additional experiments to further clarify and understand the effects of the nature of the end groups of PEG-based ligands on the long term behavior in growth media and inside live cells are in progress. Results will be detailed in future work.

Conclusion

We reported the synthesis and characterization of a new set of ligands made with poly(ethylene glycol) methyl ether (mPEG) and thioctic acid (TA), and further used them for surface modification of quantum dots (QDs) and gold nanoparticles (AuNPs). These ligands feature a more stable amide bond between TA and PEG and a methoxy-terminal group, which constitute an improvement over our previous design using an ester linkage and an OH terminal group.[17] The new ligands are chemically more stable and present a more inert terminal function. The synthesis and purification were also simplified and made more efficient by starting with a precursor that has only one reactive group, namely poly(ethylene glycol) methyl ether. In three simple and efficient reaction steps TA is coupled to mPEG, resulting in TA-PEG-OCH_3 ligands. These ligands were subsequently reduced by $NaBH_4$ to yield dithiol-terminated PEG ligands with no loss of the precursor integrity. We demonstrated the utility of DHLA-PEG-OCH_3 ligands by performing cap exchange on QDs and AuNPs to promote their dispersion in aqueous buffers and over a broad range of pHs and salt conditions. The new ligands can be combined with other reactive DHLA-PEG ligands in one cap exchange step to yield QDs with controlled fraction of reactive groups (*e.g.*, amines and COOH) on their surface. Absorption and fluorescence measurements combined with gel electrophoresis confirmed that cap exchange with both neat and mixed ligands of QDs was effective and that control over the molar fractions of surface ligands was achieved. The stability and inert nature of DHLA-PEG-OCH_3-QDs were further tested in live cells, where perinuclear dispersion of homogeneous fluorescence pattern in the cell cytosol was observed 32 h post injection, indicating that by altering the terminal group to OCH_3 non-specific interactions with the ion-rich cytoplasm could be reduced. We have also shown that the new ligands (TA- and DHLA-PEG-OCH_3) can be used to surface modify gold nanoparticles and further enhance their stability in solutions containing a high excess of counter-ions as well as in a wide range of pH conditions. These results provide an additional tool for researchers seeking more stable and versatile QDs, AuNPs and other metallic nanoparticles in biologically relevant conditions (media that are rich in salts, ions and over a broad pH range).

Acknowledgements

The authors acknowledge NRL, ONR, ARO, the NSF-IGERT(DGE-0504485) and the University of Massachusetts for financial support.

References

1 R. C. Somers, M. G. Bawendi and D. G. Nocera, *Chem. Soc. Rev.*, 2007, **36**, 579–591.
2 *Nanobiotechnology II: More Concepts and Applications*, ed. C. A. Mirkin and C. M. Niemeyer, Wiley-VCH, Darmstadt, 2007.
3 M. Zhou and I. Ghosh, *Biopolymers*, 2007, **88**, 325–339.
4 V. I. Klimov, *J. Phys. Chem. B*, 2006, **110**, 16827–16845.
5 C. B. Murray, C. R. Kagan and M. G. Bawendi, *Annu. Rev. Mater. Sci.*, 2000, **30**, 545–610.
6 X. Y. Wu, H. J. Liu, J. Q. Liu, K. N. Haley, J. A. Treadway, J. P. Larson, N. F. Ge, F. Peale and M. P. Bruchez, *Nat. Biotechnol.*, 2003, **21**, 452–452.
7 M. C. Daniel and D. Astruc, *Chem. Rev.*, 2004, **104**, 293–346.
8 I. L. Medintz, H. T. Uyeda, E. R. Goldman and H. Mattoussi, *Nat. Mater.*, 2005, **4**, 435–446.
9 J. C. Love, L. A. Estroff, J. K. Kriebel, R. G. Nuzzo and G. M. Whitesides, *Chem. Rev.*, 2005, **105**, 1103–1169.
10 X. Michalet, F. F. Pinaud, L. A. Bentolila, J. M. Tsay, S. Doose, J. J. Li, G. Sundaresan, A. M. Wu, S. S. Gambhir and S. Weiss, *Science*, 2005, **307**, 538–544.
11 M. A. Hines and P. Guyot-Sionnest, *J. Phys. Chem. B*, 1998, **102**, 3655–3657.
12 F. Pinaud, D. King, H. P. Moore and S. Weiss, *J. Am. Chem. Soc.*, 2004, **126**, 6115–6123.
13 Z. A. Peng and X. G. Peng, *J. Am. Chem. Soc.*, 2001, **123**, 183–184.
14 C. B. Murray, D. J. Norris and M. G. Bawendi, *J. Am. Chem. Soc.*, 1993, **115**, 8706–8715.
15 B. O. Dabbousi, J. Rodriguez-Viejo, F. V. Mikulec, J. R. Heine, H. Mattoussi, R. Ober, K. F. Jensen and M. G. Bawendi, *J. Phys. Chem. B*, 1997, **101**, 9463–9475.
16 A. R. Clapp, E. R. Goldman and H. Mattoussi, *Nat. Protoc.*, 2006, **1**, 1258–1266.
17 H. T. Uyeda, I. L. Medintz, J. K. Jaiswal, S. M. Simon and H. Mattoussi, *J. Am. Chem. Soc.*, 2005, **127**, 3870–3878.

18 K. Susumu, H. T. Uyeda, I. L. Medintz, T. Pons, J. B. Delehanty and H. Mattoussi, *J. Am. Chem. Soc.*, 2007, **129**, 13987–13996.
19 W. Liu, M. Howarth, A. B. Greytak, Y. Zheng, D. G. Nocera, A. Y. Ting and M. G. Bawendi, *J. Am. Chem. Soc.*, 2008, **130**, 1274–1284.
20 W. C. W. Chan and S. M. Nie, *Science*, 1998, **281**, 2016–2018.
21 B. Dubertret, P. Skourides, D. J. Norris, V. Noireaux, A. H. Brivanlou and A. Libchaber, *Science*, 2002, **298**, 1759–1762.
22 X. H. Gao, Y. Y. Cui, R. M. Levenson, L. W. K. Chung and S. M. Nie, *Nat. Biotechnol.*, 2004, **22**, 969–976.
23 C. A. J. Lin, R. A. Sperling, J. K. Li, T. Y. Yang, P. Y. Li, M. Zanella, W. H. Chang and W. G. J. Parak, *Small*, 2008, **4**, 334–341.
24 G. T. Hermanson, *Bioconjugate Techniques*, Academic Press, Inc., San Diego, 1996.
25 B. C. Mei, K. Susumu, I. L. Medintz, J. B. Delehanty and H. Mattoussi, *Proc. SPIE–Int. Sc. Opt. Eng.*, 2008, **6866**, 686606.
26 B. Ballou, B. C. Lagerholm, L. A. Ernst, M. P. Bruchez and A. S. Waggoner, *Bioconjugate Chem.*, 2004, **15**, 79–86.
27 E. L. Bentzen, I. D. Tomlinson, J. Mason, P. Gresch, M. R. Warnement, D. Wright, E. Sanders-Bush, R. Blakely and S. J. Rosenthal, *Bioconjugate Chem.*, 2005, **16**, 1488–1494.
28 C. A. Leatherdale, W. K. Woo, F. V. Mikulec and M. G. Bawendi, *J. Phys. Chem. B*, 2002, **106**, 7619–7622.
29 V. Dixit, J. Van den Bossche, D. M. Sherman, D. H. Thompson and R. P. Andres, *Bioconjugate Chem.*, 2006, **17**, 603–609.
30 R. C. Mucic, J. J. Storhoff, C. A. Mirkin and R. L. Letsinger, *J. Am. Chem. Soc.*, 1998, **120**, 12674–12675.
31 E. Koplin, C. M. Niemeyer and U. Simon, *J. Mater. Chem.*, 2006, **16**, 1338–1344.
32 J. B. Delehanty, I. L. Medintz, T. Pons, F. M. Brunel, P. E. Dawson and H. Mattoussi, *Bioconjugate Chem.*, 2006, **17**, 920–927.
33 A. W. Schwabacher, J. W. Lane, M. W. Schiesher, K. M. Leigh and C. W. Johnson, *J. Org. Chem.*, 1998, **63**, 1727–1729.
34 S. S. Iyer, A. S. Anderson, S. Reed, B. Swanson and E. G. Schmidt, *Tetrahedron Lett.*, 2004, **45**, 6207–6207.
35 R. G. Pearson, *J. Chem. Educ.*, 1968, **45**, 581–588.
36 R. G. Pearson, *J. Chem. Educ.*, 1968, **45**, 643–649.
37 B. Garcia, M. Salome, L. Lemelle, J. L. Bridot, P. Gillet, P. Perriat, S. Roux and O. Tillement, *Chem. Commun.*, 2005, 369–371.
38 J. K. Jaiswal, H. Mattoussi, J. M. Mauro and S. M. Simon, *Nat. Biotechnol.*, 2003, **21**, 47–51.